Using a SARS-CoV-2 Pseudotyped Lentivirus to Determine the Tropism in Human Lung Cell Suspensions

by

Morgan D. Ritchie

BS in Biology, Allegheny College, 2019

Submitted to the Graduate Faculty of the

School of Public Health in partial fulfillment

of the requirements for the degree of

Master of Science

University of Pittsburgh

2024

UNIVERSITY OF PITTSBURGH

SCHOOL OF PUBLIC HEALTH

This thesis was presented

by

Morgan D. Ritchie

It was defended on

June 10, 2024

and approved by

Thesis Director: Dr. Simon Barratt-Boyes, Professor, Department of Infectious Diseases and Microbiology

Committee Member: Dr. Jeremy Martinson, Assistant Professor, Department of Infectious Diseases and Microbiology

Committee Member: Dr. Yuan Liu: Assistant Professor, Department of Medicine, Institute of Aging

Using a SARS-CoV-2 Pseudotyped Lentivirus to Determine the Tropism in Human Lung Cell Suspensions

Morgan D. Ritchie, MS

University of Pittsburgh, 2024

Severe Acute Respiratory Syndrome Coronavirus 2 (SARS-CoV-2) is the novel, positive-sense RNA coronavirus was discovered in late December 2019 in Wuhan, China. This virus causes COVID-19 and was responsible for a global pandemic. There have been over 775 million cases reported worldwide, and over 7 million deaths worldwide. COVID-19 symptoms vary from person to person usually depending on age, sex, and pre-existing illnesses. Symptoms could range anywhere from a mild cold to severe pneumonia and death. The surface SARS-CoV-2 is covered with a structural spike glycoprotein, which binds to human angiotensin-converting enzyme 2 (ACE2) to infect susceptible cells. Most infection from SARS-CoV-2 takes place in epithelial cells in respiratory tract, with the main target being alveolar type II epithelial cells. While ACE2 is expressed on alveolar type II cells in the lungs, it is also expressed in the heart, kidneys, intestines, and other tissue.

Due to the SARS-CoV-2 spike protein's ability to bind to ACE2, spike is a main target for vaccine development. However, new variants are constantly circulating, which can render current vaccines and treatments less effective. SARS-CoV-2 is currently a biosafety level three pathogen, so access to work with the virus is limited and comes with a certain level of risk associated with it. My project aims to develop a SARS-CoV-2 pseudotyped lentivirus that contains the spike glycoprotein from the Wuhan strain of SARS-CoV-2 and identify which cells in human lung cell suspensions are infected using microscopic fluorescent imaging and flow cytometry. We have

observed that developing a pseudotyped lentivirus with the Wuhan SARS-CoV-2 spike protein is possible, but efficiency of the virus varies between cell lines and between different donors. Future steps will be needed to improve the efficiency of the pseudotyped virus.

Table of Contents

Preface xi

1.0 Introduction: Severe Acute Respiratory Syndrome Coronavirus 2 1

1.1 SARS-CoV-2 Background 2

1.1.1 Spike Protein Structure 3

1.1.2 Viral Entry and Replication 4

1.1.3 Current State of Pandemic 5

1.2 Human Lungs and COVID-19 9

1.2.1 The Human Lungs 9

1.2.2 Angiotensin-Converting Enzyme 2 (ACE2) 10

1.2.3 SARS-CoV-2 and Comorbidities 11

1.3 Pseudotyped Lentiviruses 12

2.0 Specific Aims 14

3.0 Methods 16

3.1 Human Lung Cell Suspensions 16

3.2 Vero E6 and 293T Growth and Maintenance 17

3.3* Transforming *E. coli 17

3.4 DNA Plasmid Purification 18

3.5 Transfection 19

3.6 Preparing PEG Precipitation 20

3.7 Infection of Vero E6 and 293T ACE2/TMPRSS2 Cells 20

3.8 Infection of Human Lung Cell Suspensions 21

3.9 Preparing Slides and Immunofluorescence Staining 21

3.10 Imaging with EVOS M5000 Fluorescence Microscope 22

3.11 Flow Cytometry 23

4.0 Results 25

4.1 Aim 1: Generate a Wuhan Strain SARS-CoV-2 Pseudotyped Lentivirus Capable of Infecting Human Lung Cells in Suspension 25

4.1.1 Infection of Vero E6 ACE2/TMPRSS2 to Understand Efficiency of SARS-CoV-2 Pseudotyped Lentivirus 25

4.1.2 Infection of 293T Cells that Express Human ACE2/TMPRSS2 to Understand Viral Efficiency 27

4.2 Aim 2: The infection of Human Lung Cell Suspensions with the Wuhan Strain SARS-CoV-2 Pseudotyped Lentivirus 30

4.2.1 Microscopic Imaging and Flow Cytometry of Human Lung Cell Suspensions Infected with the SARS-CoV-2 Pseudotyped Lentivirus 30

5.0 Discussion 41

6.0 Future Directions 45

7.0 Public Health Significance 46

Bibliography 47

List of Tables

Table 1 Antibodies Used for Flow Cytometry 24

Table 2 Human Lung Donor Information 30

List of Figures

Figure 1 Mechanism of SARS-CoV-2 Viral Entry..... 4

Figure 2 Total Number of Provisional COVID-19 Deaths in the United States 6

Figure 3 Protocol for Generating SARS-CoV-2 Pseudotyped Lentivirus 13

Figure 4 Infection of Vero E6 Cells that Express Human ACE2/TMPRSS2..... 26

Figure 5 Flow Cytometry Vero E6 Cells Expressing ACE2/TMPRSS2 27

Figure 6 Infection of 293T Cells that Express Human ACE2/TMPRSS2 29

Figure 7 Flow Cytometry 293T Cells Expressing ACE2/TMPRSS2 30

Figure 8 Infection of Human Lung Cell Suspensions..... 32

Figure 9 mCherry Positive Cell Density in Human Lung Cell Suspensions 32

Figure 10 Infection of Human Lung Cell Suspensions and ACE2 Staining..... 33

Figure 11 ACE2 Expression in Human Lung Cell Suspensions Infected with SARS-CoV-2 Pseudotyped Lentivirus..... 34

Figure 12 Flow Cytometry on Uninfected Human Lung Cell Suspensions..... 35

Figure 13 Populaiton Percentages of Uninfected Human Lung Cell Suspensions..... 36

Figure 14 Flow Cytometry Human Lung Cell Suspensions Infected with SARS-CoV-2 Pseudotyped Lentivirus..... 37

Figure 15 Populaiton Percentages of Infected Human Lung Cell Suspensions 37

Figure 16 mCherry Signal Using Flow Cytometry in Human Lung Cell Suspensions Infected with SARS-CoV-2 Pseudotyped Lentivirus..... 38

Figure 17 EpCAM+mCherry+ Percentages of Infected Human Lung Cell Suspensions.... 39

Figure 18 mCherry Population Comparisons Using Flow Cytometry 40

Figure 19 mCherry Population Comparisons Between Donors 40

Preface

First, I would like to thank Dr. Barratt-Boyes, our laboratory group, and my colleagues at Quest Diagnostics. Thank you all for your patience and kind words along the way that made this possible for me. I have learned so much over the past few years, and I have truly been pushed to better myself in order to become a better scientist and public health advocate. I would also like to thank Dr. Jeremy Martinson and Dr. Yuan Liu for their mentorship and guidance on this project. I could not have received better mentors. Lastly, I would like to thank my friends, family, and fiancé who have supported me on this journey and will continue to do so as I go forth into the public health field.

1.0 Introduction: Severe Acute Respiratory Syndrome Coronavirus 2

Several cases of pneumonia of started occurring in Wuhan, China in late December of 2019, which was a cause for concern because the origin of the cases was unknown (1). More cases were being reported, and by January 2020, the causative agent was identified as Severe Acute Respiratory Syndrome Coronavirus 2 (SARS-CoV-2), and the disease was termed Coronavirus Disease-19 (COVID-19). By March 2020, the World Health Organization declared the state of COVID-19 had reached pandemic level, and the world was forever altered (1). SARS-CoV-2 is an enveloped virus with a lipid membrane that is covered with a spike glycoprotein that attaches to host cell receptors (1). Symptoms vary from person to person but typically include fever or chills, cough, shortness of breath, fatigue, and muscle aches. However, symptoms can progress to severe pneumonia, multiple organ failure, and even death (2).

The surface glycoprotein of SARS-CoV-2, spike, is composed of two subunits, S1 and S2 (3). S1 binds to Angiotensin-converting enzyme 2 (ACE2) on susceptible host cells, and S2 connects spike to the host cell membrane to begin membrane fusion. This allows for the viral genome to reach the cytoplasm, so the virus can begin replication (3). Spike is both necessary and sufficient for binding to the host cell which leads to replication, so it is a major target for the development of therapeutics and vaccines (3).

SARS-CoV-2 is currently a biosafety level three pathogen, so to work with this virus, high containment facilities, government clearances, and highly trained personal are required. Pseudotyping lentiviral particles with the spike glycoprotein of SARS-CoV-2 circumvents some of these requirements by making a reliable model that is replication incompetent (4). This study aims to create a Wuhan strain SARS-CoV-2 pseudotyped lentivirus that is capable of infecting

human lung cells in suspension and identify the tropism of the pseudotyped lentivirus using techniques such as microscopic fluorescent imaging and flow cytometry. We hypothesize that the Wuhan strain SARS-CoV-2 will be a reliable method of studying SARS-CoV-2, and it will infect epithelial cells in human lung cell suspensions that express ACE2, specifically alveolar type II cells.

1.1 SARS-CoV-2 Background

Severe acute respiratory syndrome coronavirus 2 (SARS-CoV-2) was first discovered in Wuhan, China in 2019, and it is responsible for coronavirus disease-19 (COVID-19) (2). SARS-CoV-2 belongs to the genus betacoronavirus and is an enveloped virus with a lipid membrane covered with spike glycoproteins giving it the crown like structure for which the family of viruses is named after (1,5). The virus is a positive sense single stranded RNA virus with a genome of approximately 30kb and is made up of several proteins including spike protein, envelope protein, membrane protein, and a nucleocapsid protein (6).

It is thought that SARS-CoV-2 originated in bats. The virus shares a high degree of sequence identity with the bat coronavirus and SARS-CoV, which bats are the known natural reservoir (7). SARS-CoV, MERS, and SARS-CoV-2 proven that coronavirus have the capability to cross species barriers and infect humans. Person to person transmission is sustained with SARS-CoV-2, and respiratory droplets are the main route (7,8).

1.1.1 Spike Protein Structure

The spike protein of SARS-CoV-2 is a type one membrane protein meaning the protein's transmembrane domain is situated so the amino terminus is expressed on the extracellular side of the membrane (3). The full length of the spike of the Wuhan strain has 1273 amino acid residues and includes the N terminus signal peptide, receptor binding fragment S1, and fusion fragment S2 (9). S1 is composed of the N-terminal domain, receptor binding domain and C-terminal domains 1 and 2 and is used to bind to the receptors on susceptible host cells and anchor to the surface. S2 includes fusion peptides, fusion peptide proximal region, heptad repeat 1 and 2, central helix, connector domain, transmembrane segment, and the cytoplasmic tail. The main function of S2 is membrane fusion (3, 9). The main host receptor for spike is angiotensin-converting enzyme 2 (ACE2), and when spike binds to ACE2, it undergoes structural rearrangement. This allows the virus to begin membrane fusion to enter the cytoplasm (9).

1.1.2 Viral Entry and Replication

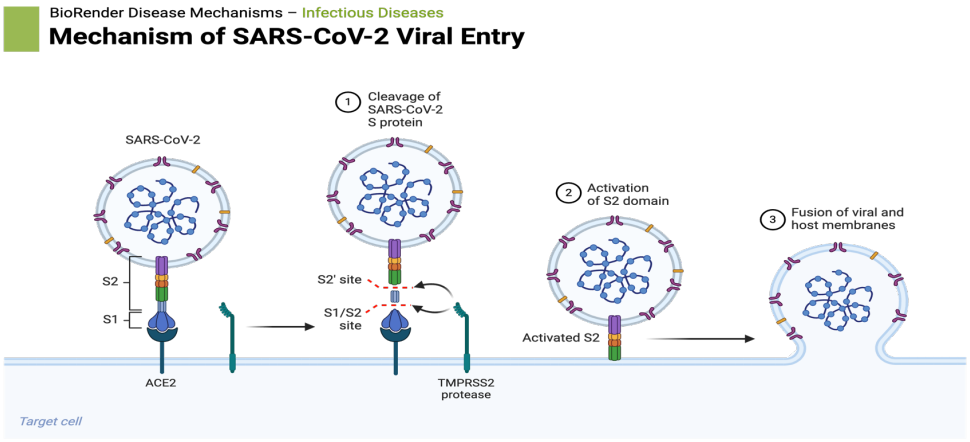

Figure 1 Mechanism of SARS-CoV-2 Viral Entry

Diagram depicting viral entry into a host cell. Spike protein engages with host ACE2 and is cleaved at the S1/S2 sites by TMPRSS2. S2 becomes activated and drives fusion of viral and host membranes. Created with Biorender.com and obtained with permission from Journal of Biological Chemistry (2020) 295:12910-12934.

SARS-CoV-2 spike protein is necessary and sufficient for binding to the host cell receptor ACE2. Spike binds to ACE2 and is cleaved by TMPRSS2 then fuses with the host cell membrane to deposit the RNA genome (Figure 1). The positive sense RNA can directly begin production of viral proteins to assemble the RNA dependent RNA polymerase (RdRp) complex (10,11). The RdRp uses the genome as a template to generate a negative sense subgenome and genome length RNAs to begin synthesis of the positive sense progeny genomes. Transcription and replication then take place and the subgenomic mRNAs are translated into structural and accessory proteins. The genomic RNA is bound by the nucleocapsid and then buds into the ERGIC. The enveloped virus is then complete and expelled from the host cell by exocytosis (10,11).

1.1.3 Current State of Pandemic

As of May 12, 2024, there have been over 775 million cases of COVID-19 reported worldwide, with 103 million of those cases occurring in the United States (Figure 2). There has been over 7 million deaths from COVID-19, and 1.2 million of those deaths have occurred in the United States (12). The first case in the United States was reported on January 21, 2020, and the virus quickly spread from there (13).

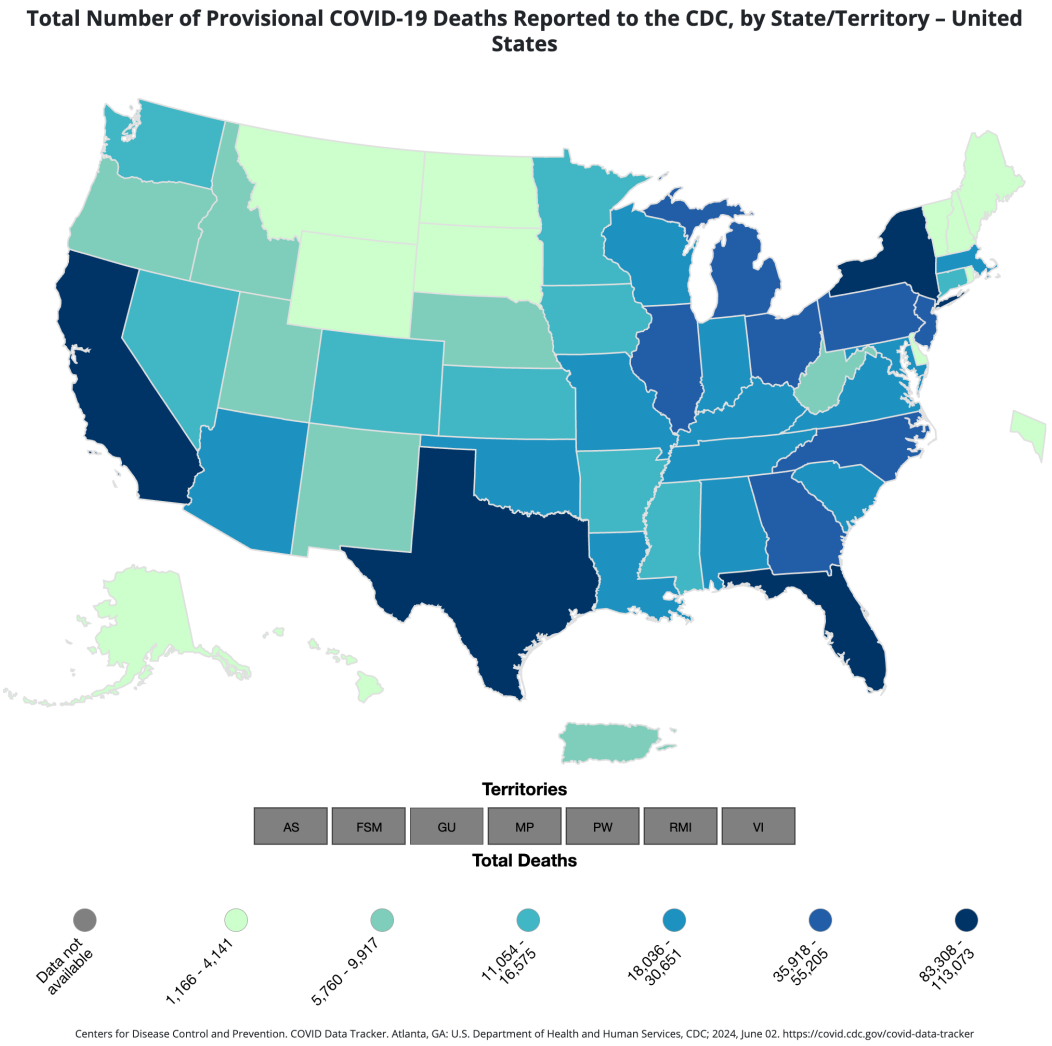

Figure 2 Total Number of Provisional COVID-19 Deaths in the United States

Map depicting the number of COVID-19 deaths in the United States reported to the CDC since January 1, 2020, by state/territory. Obtained with permission from the Center for Disease Control.

Symptoms of COVID-19 can vary from person to person depending upon several factors like age, sex, race, and prior health status. Individuals over the age of 60 are at elevated risk for disease, and typically there are more cases in males (14). Symptoms typically include fever or chills, cough, and body aches, but can progress to severe pneumonia, neurological symptoms, multiple organ failure and death (14,15). The incubation period of COVID-19 is anywhere from

2-14 days after exposure to symptom onset, with an average of about 5 days (16). Some individuals will test positive but remain asymptomatic, while others develop Long COVID and experience symptoms for weeks after a negative PCR test for the virus (15). Still little is known about the prevalence and risk factors of Long COVID. Individuals are more likely to experience Long COVID with increased age, the female sex, and increased body mass (17).

There are several factors at play that keeps SARS-CoV-2 circulating. It still is not completely understood how pre-symptomatic and asymptomatic spread contributions to circulation. It is estimated that 25-40% of transmission occurs before the onset of symptoms (18). The extent of asymptomatic cases remains unclear for several reasons. There is still inconsistent symptom reporting, inadequate follow up time with physicians and incomplete assessments, and a general lack of reporting cases (18). Due to the difficulties addressing asymptomatic cases, it is hard to estimate the proportion of these cases (19).

As the virus continues to circulate in the population, there is an increased chance that the virus will mutate, and variants will arise. All viruses mutate as they replicate and spread, but RNA viruses mutate faster than DNA viruses (20). The variant strains of SARS-CoV-2 may have different abilities in terms of how quickly they spread or the severity of illness they cause, and they may even decrease the effectiveness of therapeutics and vaccines (20). Notable strains have been the Wuhan strain, Delta, and Omicron. The newest variant circulating is from the Pango lineage, KP3, and the most prevalent as of May 12, 2024, is the JN1 variant (21). The JN1 variant is responsible for approximately 64.26% of reported cases in the last 28 days (21).

Fortunately, there are vaccines and therapeutics available to help prevent and treat COVID-19. The Center for Disease Control recommends Pfizer-BioNTech, Moderna, and Novavax vaccines. They recommend everyone aged 5 years and older should get 1 dose of an updated

COVID-19 vaccine, and the general population should follow vaccine recommendations for receiving boosters. Immunocompromised patients may require an additional dosage (22). Despite evidence that these vaccines are effective in protecting individuals from severe disease and hospitalization, there is still a large population worldwide that remains unvaccinated, which according to the World Health Organization is a top 10 threat to global health (23). There are many reasons for an individual to be hesitant to receive a vaccine like race, sex, and religious beliefs, but unfortunately, a main reason to be hesitant is lack in faith of the health care system and government measures (23,24). Understanding this virus better would allow for more open communication about vaccines and could decrease hesitancy worldwide.

Additionally, there are some therapeutic options. There is pre-exposure prophylaxis, or preventative monoclonal antibodies, which is an intravenous treatment for immunocompromised or elderly patients. There are multiple drug options including Paxlovid and Lageviro (25). Paxlovid is a combination of Nirmatrelvir and Ritonavir. It is an oral medication that targets key enzymes that SARS-CoV-2 requires for replication (26). This medication is associated with lower hospitalization and mortality rates (26). However, the prevalence of COVID-19 rebound needs to be studied further for people using these medications, and the efficacy is still controversial and potentially compromised by variants (27).

1.2 Human Lungs and COVID-19

1.2.1 The Human Lungs

The human lungs are a complex organ primarily used for gas exchange between the body and its environment. Air flows in through the nasal cavity and to the trachea and main bronchi to the bronchial tree. The airways eventually end in the terminal bronchioles which lead to respiratory units like alveolar ducts and sacs (28). There are three main components of the lung, airway cells in the bronchial and bronchiolar epithelium, alveolar unit cells, and pulmonary vascular cells. Airway cells include basal, secretory, and ciliated cells. Alveolar unit cells are type I and type II alveolar cells. Both groups are composed of epithelial cells (28,29). Lastly, the pulmonary vascular cells are endothelial cells from different vascular structures (29).

Recent analysis has revealed that there are 58 unique cell types in the human lungs (30). These cells can be broken down into five main categories. Alveolar type I epithelial cells make up 8% of the cell population and are some of the largest cells in the lung, while alveolar type II epithelial cells account for 7% of the cell population (31). Capillary endothelial cells are about 30% of the total lung population, but they are much smaller in size. Interstitial space cells account for 37% of the lung population, and the total for alveolar macrophages ranges anywhere from 3-19% depending upon the individual (31).

The alveolar surface is composed of the type I and type II alveolar epithelium cells. Alveolar type I cells are large flat cells that cover 95% of the alveolar surface (32). This is where gas exchange happens in the lungs (32,33). Alveolar type II cells are smaller lamellar bodies. They make and secrete pulmonary surfactant, restore epithelium when there is damage to the alveolar

type I cells, transport sodium and fluids, and play a major role in the innate immune response (32,33).

Alveolar type II cells are considered the defenders of the alveolus due to their key participation in the innate immune function in response to inhaled materials and microorganisms. The surfactant that alveolar type II cells produce creates a low surface tension to facilitate gas exchange and also has antimicrobial and anti-inflammatory properties (34). This helps defend the cells from constant exposure of inhaled particles while not causing constant inflammation which would lead to fluid buildup in the lungs (34). The alveolar type II cells, along with many other cells in the human body, are known to express ACE2 (35). The location and expression of the alveolar type II cells makes them extremely susceptible to SARS-CoV-2 (36).

1.2.2 Angiotensin-Converting Enzyme 2 (ACE2)

Angiotensin-converting enzyme 2 (ACE2) is a membrane receptor found on the surface of cells in the lungs, heart, kidneys, intestines, and other tissues in the human body. Expression levels of ACE2 vary from cell to cell and from person to person (37). Age, sex, ethnicity, medication usage, and other comorbidities are all determinates of ACE2 expression (38). TMPRSS2 and ACE2 expression are typically expressed on the same cell types (39).

ACE2 plays major roles in regulating the kinin-kallikrein system (KKS), renin-angiotensin system (RAAS), and coagulation systems (39). In KKS, ACE2 drives the bradykinin metabolism by inactivating des-Arg9 bradykinin which inhibits vasodilation and leads to the elevation of vascular permeability (38). ACE and ACE2 also regulate Kallikrein enzymes bradykinin I and DABK respectively, and an increase in DABK can lead to increased respiratory disease severity (40).

In RAAS, angiotensinogen is produced by the liver, and cleaved by renin which forms angiotensin I (Ang I). ACE converts Ang I to Ang II. Ang II is a main component in vasocontraction and blood pressure elevation. ACE2 cleaves Ang II to angiotensin (1-7), which is responsible for vasodilation (38,41). Ang (1-7) counterbalances vasoconstriction and pro-inflammatory and pro-coagulation response (42).

Additionally, ACE2 is the main target for SARS-CoV-2 infection. The spike glycoprotein uses ACE2 to mediate entry into the host cell (43). SARS-CoV-2 has a 10-20-fold increase affinity to ACE2 compared to SARS-CoV. Infection with SARS-CoV-2 can lead to downregulation of ACE2 and cause problems throughout the human body (38).

1.2.3 SARS-CoV-2 and Comorbidities

The impacts of COVID-19 on the lungs are very apparent in disease manifestation, but the damage to other organs is not always clear. While individuals with comorbidities are not more susceptible to SARS-CoV-2, they are more likely to develop severe COVID-19. There is an increased prevalence of patients with obesity, diabetes, and cardiovascular disease being hospitalized for COVID-19 (44). It is known that ACE2 is expressed on the pancreas, but the effects of diabetes on ACE2 expression are not fully understood. However, some research suggest that the hyperglycemic condition of diabetic patients can increase the virulence of SARS-CoV-2 (45). In hypertension, patients that develop COVID-19 have a 3.48-fold higher risk of fatality compared to patients that do not have hypertension. It is believed that the downregulation of ACE2 during SARS-CoV-2 infection disrupts the balance of the RAAS system leading to overactivation of ACE and Ang II causing tissue damage (46). Thrombosis in COVID-19 patients has also been noted. The innate immune response actives upon initial infection, and coagulation happens soon

after to localize the infection. However, if there is a disruption to the RAAS system and not enough ACE2 to regulate it, too much coagulation could occur (47). SARS-CoV-2 infection is linked to elevated D-Dimer which leads to thrombosis (48).

1.3 Pseudotyped Lentiviruses

Due to the severity of SARS-CoV-2 and how quickly it can spread, it is currently classified as a biosafety level 3 pathogen. The spike glycoprotein on the surface of the virus is both necessary and sufficient for binding and entry to host cells making it an ideal target for therapeutics, vaccines, and other research (4). It is possible to pseudotype the SARS-CoV-2 spike onto lentiviral particles to create a reliable model for studying SARS-CoV-2 in a safer, lower containment level setting. Pseudotyped lentiviruses are replication incompetent, which allows for little to no risk while working with this virus (49). Pseudotyped lentiviruses have been used for many deadly viruses, including Ebola, H5N1, and rabies, and it has been proven in many studies to be a reliable and effective model to assist in understanding cellular interactions, therapeutics, vaccines, and even gene therapy (50,51). This model allows researchers in lower-level containment and funding laboratories to research viruses that would need high level containment facilities. They would no longer require government clearances or specialized training, or specific equipment to study SARS-CoV-2 (52). Pseudotyping the spike protein from the Wuhan strain of SARS-CoV-2 onto a lentivirus containing mCherry, a fluorescent protein, has been determined to be a reliable model for studying SARS-CoV-2 (52). Our laboratory plans to utilize this model to create a Wuhan strain SARS-CoV-2 pseudotyped lentivirus and determine the tropism in human lung cell suspensions using fluorescent microscopic imaging and flow cytometry (Figure 3). We used the SARS-Related

Coronavirus 2, Wuhan-Hu-1 Spike-Pseudotyped Lentiviral Kit V2 from BEI resource (NR-53816), pLv-mCherry plasmid (#36084) from Addgene, BioT transfection kit from Bioland Scientific to create the SARS-CoV-2 pseudotyped lentivirus.

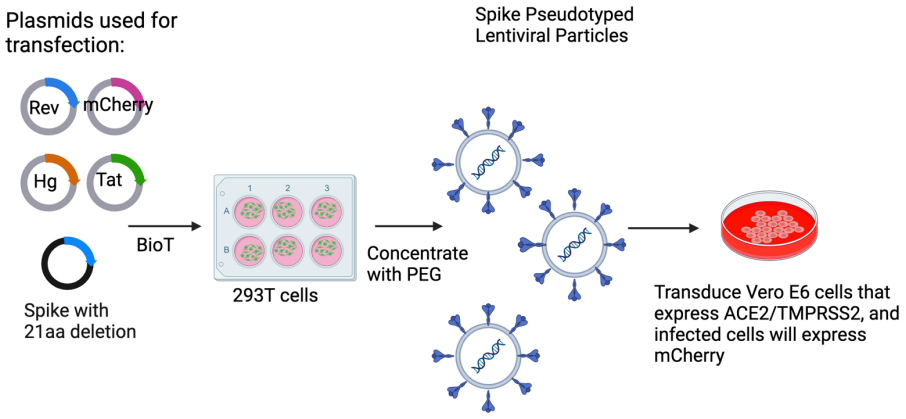

Figure 3 Protocol for Generating SARS-CoV-2 Pseudotyped Lentivirus

Diagram depicting simplified protocol for pseudotying the Wuhan stain SARS-CoV-2 spike protein onto lentiviral particles to make viral particles that are capable of infecting cells that express ACE2/TMPRSS2. First, prepare the plasmids needed and transfect 293T cells then concentrate using PEG. Infect susceptible cells to check efficiency of viral particles. Created with Biorender.com.

2.0 Specific Aims

The unprecedented impact that SARS-CoV-2 and COVID-19 had on the world was devastating, and with the emergence of new variants, it is clear that this virus is here to stay. The proposed study will aim to create a working SARS-CoV-2 pseudotyped lentivirus capable of infecting human lung cells in suspension and identify which cells are infected by observing which cells are expressing mCherry signal using microscopic fluorescent imaging and flow cytometry. This creates a more accessible and cost-effective way to study SARS-CoV-2 because pseudotyped viruses are replication incompetent and can be handled in a biosafety level two setting. Infecting human lung cell suspensions and observing infection will show that using a pseudotyped lentivirus is a reliable method to study SARS-CoV-2.

Aim 1: Generate a Wuhan strain SARS-CoV-2 pseudotyped lentivirus capable of infecting human lung cells in suspension

A. Transfect the SARS-CoV-2 spike protein with lentiviral backbone and helper plasmids

B. Include fluorescent marker, mCherry, in viral particles to indicate infection inside of susceptible cells

C. Infect susceptible cell lines, Vero E6 and 293T cells that express human ACE2, to check efficiency of the pseudotyped virus

Aim 2: Determine tropism of the pseudotyped lentivirus in human lung cell suspensions

A. Microscopic imaging on susceptible cell lines and human lung cell suspensions infected with the SARS-CoV-2 pseudotyped lentivirus

B. Flow cytometry analysis of infected cell lines and human lung cell suspensions

Hypothesis:

If the Wuhan strain SARS-CoV-2 spike protein can be pseudotyped onto lentiviral particles, then we will be able to infect susceptible cell lines, and there will be infection in human lung cell suspensions, specifically in epithelial cells, because the pseudotyped virus binds to ACE2, demonstrating that this model is a functional and reliable method to study SARS-CoV-2.

3.0 Methods

3.1 Human Lung Cell Suspensions

All donors were specimens rejected for transplantation and received from The International Institute for the Advancement of Medicine in 2021 and processed before this study began and stored in liquid nitrogen storage at 180°C. A small amount of lung digestion media was poured into a 150mm tissue culture dish with lung, then it was cut into small 1cm by 1cm chunks using scissors and forceps. Pieces were placed into 50mL conical tubes and filled with digestion media. Samples were incubated at 37°C for 30-45 minutes and 5-6 conical tubes were prepared with 10mL FBS. A 70µm cell strainer was placed on top of each conical. After incubation period, the contents were poured from the conical tubes into a Bellco collector sieve sitting in a 150mm petri dish, and the tissue was mashed with a 5mL syringe plunger. The samples were washed with digestion buffer and transferred liquid to the 70µm cell strainers. Only 35-40mL were placed in each conical tube, and then they were inverted to mix once closed. Samples were centrifuged at 2,000rpm for 10 minutes at 4°C, then sat to incubate at room temperature for 5-10 minutes. We then filled the conical tubes to 50mL with 1X PBS and centrifuged at 2,000rpm for 10 minutes at 4°C. The supernatant was carefully decanted, and the pellet was resuspended in 40mL of MACS buffer, then centrifuged again at 2,000rpm for 10 minutes at 4°C. The supernatant was decanted and resuspended in calculated amount of freezing media. The samples were aliquoted into 1mL liquid nitrogen cyrovials and placed into Mr. Frosty containers. They were left in -80°C for 24 hours before transferring to the liquid nitrogen freezer.

3.2 Vero E6 and 293T Growth and Maintenance

Cells are stored in liquid nitrogen and were quick thaw in 37°C water bath. Conical tubes containing 14mL of Vero E6 media were prepared, and then add the cells to the conical tube. The the conical tubes were spun in the centrifuge at 4°C 800xg for 10 minutes. The supernatant was decanted, and the pellet was resuspended in 8mL of Vero E6 media. For Vero E6 cells that express human ACE2/TMPRSS2 puromycin was added and for 293T cells that express human ACE2/TMPRSS2 zeocin was added both at a 1:1,000 ratio every time the cells are split. Cells were placed into a T25 flask and stored in 37°C incubator.

Once the monolayer is 80-90% confluent, the cells were split and added to a larger flask by discarding the media from the flask and rising with 1X PBS. Trypsin-EDTA was added to the flask and rocked the flask to cover the monolayer and flask was placed back in the 37°C incubator for 5 minutes. Once cells are detached 10mL of Vero E6 media was added to the flask and mixed to detach as many cells as possible. For a 1:6 dilution, take 5mL from the T25 flask and place into a T175 flask and add 30mL of Vero E6 media and puromycin or zeocin if needed. Flasks were placed back into the 37°C incubator.

3.3 Transforming *E. coli*

One Shot TOP10 Chemically Competent *E. coli* (C4040-10) were used. Selective LB agar plates were placed in a 37°C for at least 30 minutes before using them and S.O.C. medium was brought to room temperature. The transformation efficiency was calculated using the equation in the protocol from kit. For every transformation, one vial of *E. coli* was thawed on ice and 1-5μL

of DNA was added into vial and gently mixed. The sampled were incubated on ice for 30 minutes, then heat shocked for 30 seconds at 42°C, then placed on ice for 2 minutes. We then added 250μL S.O.C. medium to each transformation vial and shook horizontally at 37°C for 1 hour at 225rpm. Next, we spread 20-200μL of each transformation onto the selective LB agar plates. It is recommended to use two different volumes and the pUC-19 control to ensure well-spaced colonies. Any remaining transformation mix can be stored at 4°C overnight and plated the next day, if desired. Plates with transformations were left inverted in 37°C incubator overnight and select colonies the next day.

3.4 DNA Plasmid Purification

The Macherey-Nagel Plasmid DNA purification kit and protocol for the high copy plasmid purification (maxi) was used during this experiment. From the *E. coli* colonies selected from the transformations, we inoculated a 3-5mL culture of LB medium with a single colony. The samples were then shaken at 37°C and 300rpm for 8 hours. The starter culture was diluted 1:1,000 into LB medium and the appropriate selective antibiotic was added. Samples were shaken at 37°C at 300rpm for 12-16 hours. Next we centrifuge cells at 4,500-6,000g for 10 minutes at 4°C and completely removed supernatant and resuspend the pellet in 12mL resuspension buffer + RNanse A. Then we added 12mL cell lysis buffer to the suspension and gently inverted 5 times. Samples were incubated at room temperature for 5 minutes. While incubating, the Nucleobond Xtra Columns were prepared by applying 25mL equilibration buffer directly to the column filter rim. After incubation period, we added 12mL neutralization buffer and immediately inverted tube until

the sample becomes colorless. Once sample is mixed, sample was added to column filter and allowed to empty by flow of gravity. The first wash step was completed by applying 15mL equilibrium buffer to rim of filter to wash out the remaining lysate. The filter was removed, and the second wash step was done by adding 25mL of the wash buffer to the column, and the waste was discarded. 15mL of elution buffer was added to column and the eluate was collected. 10.5mL room temperature isopropanol was added to the eluted plasmid DNA and vortexed. The sample was then centrifuged at 4,500g for at least 15 minutes at 4°C then supernatant was discarded, and the pellet was resuspended in in 4mL room temperature 70% ethanol. The sample was centrifuged again at 4,500g for 5 minutes at 18-25°C and the pellet was left to dry. Pellet was reconstituted in ~1mL buffer TE and we determined plasmid yield by spectrometry.

3.5 Transfection

For this project, we used SARS-Related Coronavirus 2, Wuhan-Hu-1 Spike-Pseudotyped Lentiviral Kit V2 from BEI resource (NR-53816), pLv-mCherry plasmid (#36084) from Addgene, BioT transfection kit from Bioland Scientific. The Lentiviral kit contains Wuhan-Hu-1 spike protein with 21aa deletion, Δspike (#NR-53742), and helper plasmids, Tat1b, Rev1b, and Hgprm2 (#NR-52517, #NR-52518, #NR-52519). Confluent flasks of 293T cells and Vero E6 cells that express ACE2/TMPRSS2 were also needed.

First, we seeded 293T cells in growth media in 6-well plates. They were at least 50-75% confluent before continuing. Once confluent enough, 1μg pLv-mCherry, 0.22μg each of Tat1b, Rev1b, and Hgprm2 plasmids, 0.34μg of the Δspike plasmid, 100μg of DMEM, and 3μL of BioT in proportion to total number of wells needed were combined into a 15 mL sterile conical tube.

100μL of this mixture was placed into each well containing media in a circular motion while gently titling plate to completely mixed. After 18-24 hours post-transfection, the media was changed with fresh, pre-warmed media. 48-60 hours post-transfection, cells were observed under EVOS fluorescence microscope to make sure 80-90% of cells were expressing mCherry signal and then we transferred supernatants from transfected cells into conical tubes and centrifuge at 2,000RPM for 10 minutes at 4°C. The supernatant was filtered through 0.45μM filters. Once filtered, we mixed one part 50% PEG 3350 solution to four parts of supernatant containing pseudotyped lentivirus, and stored overnight at 4°C. After 24-72 hours, we transferred mixture to 15mL conical tubes and centrifuged at 2600RPM for 30 minutes at 4°C, then decanted supernatant into waste. The pellet was resuspended in 1/1,000 of the original volume with DMEM containing 25mM HEPES then aliquot 50mL into screw-top tubes and stored at -80°C.

3.6 Preparing PEG Precipitation

20g PEG 3350 powder was placed into 100mL glass autoclavable bottle and autoclaved for 10 minutes without pressure to melt PEG powder. While the powder is still hot, we mixed in 20 mL of DMEM media. PEG solution was kept light protected and stored at room temperature.

3.7 Infection of Vero E6 and 293T ACE2/TMPRSS2 Cells

To test the SARS-CoV-2 pseudotyped lentivirus, we used two permissible cell lines. This experiment was performed on Vero E6 and 293T cells that artificially express human

ACE2/TMPRSS2. Cells were at least 80% confluent in a 12-well plate before beginning. Frozen virus was thawed in 37°C water bath. Media was removed from wells and 100μL virus was added to each well carefully in a circular motion to not disrupt the monolayer. Peak mCherry expression was observed at 48 hours post infection.

3.8 Infection of Human Lung Cell Suspensions

Twenty-four hours before infection, we thawed one vial of human lung cell suspensions that were frozen in liquid nitrogen. The cells were washed with lung slice media and centrifuged at 300g for 5 minutes. We removed supernatant and resuspended the pellet in 2mL of fresh lung slice media and distributed equally into 4 wells of a 24-well low binding plate. The next day, all cells were removed from 24-well low binding plate and placed into a 15mL conical tube and centrifuged at 300g for 5 minutes and discarded the supernatant. Frozen virus was thawed in 37°C water bath and the pellet was resuspended in 50μL of undiluted virus. The samples incubated for an hour, while gently mixing every 15 minutes. After incubation, we added fresh, pre-warmed lung slice media and placed into a new 24-well low binding plate. Peak infection was observed at 48 hours post infection.

3.9 Preparing Slides and Immunofluorescence Staining

At 48 hours post-infection, cells were collected and centrifuged at 500g for 5 minutes at 4°C. The pellet was resuspended in 800-900μL of 2% PFA for 15 minutes at 4°C. The cytospin

slides were set with the frosted side up in the clip and the funnel filter paper side down in the clip and 100μL of sample was placed into funnel. Slides were spun at 1500rpm for 2 minutes. After removing slides from cytospin clips, the slides were set aside to dry for 15 minutes.

After slides are dry, a hydrophobic marker was used to draw a barrier around sample and the sample was rehydrated with 100μL of PBS. The PBS was removed, and the sample was permeabilized by adding 100μL of 0.1% trition-X in 1x PBS for 10 minutes. The we washed 3 times with 1x PBS and blocked with 100μL of1%BSA/PBS +1μL of Fc Block for 30 minutes, then washed 3 more times with 1x PBS. We added 100μL 1XPBS and 2μL of primary staining antibody (ACE2) to each slide and let sit for an hour in a humidified cassette. Then the primary stain was removed, and the sample was washed with washing buffer 3 times. Dapi stain was placed on the sample for 30 seconds then washed with 1x PBS 3 times. Slides were transferred to slide case and 1 drop of Prolonged Diamond was added and coverslip was placed.

3.10 Imaging with EVOS M5000 Fluorescence Microscope

Images for Vero E6 and 293T cells were taken in a 12-well plate, and human lung cell suspensions were taken from cytospin slides. The focus was adjusted on sample using the brightfield setting. Once in focus, we switched between dapi, Texas Red, and Cy5 settings, adjusting focus to match the brightfield. Starting on top edge of sample or well, we then carefully worked the whole way across and down sample area ensuring no overlap while capturing images in all color fields and overlay. NIS Elements was used to calculate area of sample expressing each stain.

3.11 Flow Cytometry

All cells were removed from 12-well plate or samples were obtained from liquid nitrogen storage, and quick thawed in 37°C water bath without letting the seal of the vial touch the water. In a 15mL conical tube 10mL of R10 media, 100µL of DNaseI and sample were combined. The samples were spun in the centrifuge at 2,000rpm for 5 minutes at 4°C. The supernatant was poured off and the remaining liquid at the bottom of the conical tube was transferred into predetermined wells in a 96-well V bottom plate. We centrifuged plate at 4°C 2,000rpm for 5 minutes then washed twice with 200µL of MACS buffer spinning in centrifuge under the same conditions each time. The pellets were resuspended in 50mL MACS buffer and antibody conditions. The antibodies used included HLA-DR BUV395, CD45 AF488, Human ACE2 AF647, EpCAM BV421, and CD163 PerCP-Cy5.5 (Table 1). The samples were then incubated in the dark at 4°C for 30 minutes. While incubating the plate, we placed 200µL of cells on a hot plate for 5-10 minutes to heat kill then added back to dead well for staining. After incubation period, 100µL of MACS buffer was added to each well and spun at 2,000rpm for 5 minutes at 4°C. The samples were rinsed with 200µL and centrifuged. The pellets were resuspened in 100µL of Live/Dead stain diluted 1:2,000 in PBS and incubated in the dark for 15 minutes at 4°C. After incubation period we added 100µL MACS buffer and centrifuged at 2,000rpm for 5 minutes at 4°C. The samples were rinsed again with 200µL MACS buffer. After spinning, the pellets were resuspended in 100µL of 2% PFA and incubated for 20 minutes. Then we rinsed twice, first with 100µL of MACS buffer and then 200µL MACS buffer and centrifuged at 2,000rpm for 5 minutes at 4°C. The pellets were resuspended in 200µL of MACS buffer and transferred to FACS tubes with an additional 100µL of MACS buffer.

Before starting analysis of samples, compensation tubes were made. An antibody with the fluorochrome PE-CF 594 was used to compensate for infection. In FACS tubes, 200µL of MACS buffer was added with 1µL of specific antibody and a drop of positive and negative beads. The FACS tube were vortexed well and incubated while adjusting settings on cytometer. While working with human lung cell suspensions is important to compensate for autofluorescence in the sample by using the AutoF function on the cytometer. All results were analyzed using FlowJo.

Table 1 Antibodies Used for Flow Cytometry

Antibody	Species	Function	Brand	Cell Populations
Live Dead	Human	Distinguish Live/Dead Cell Populations	Thermo Fisher Scientific	All Live Cells in the Sample
CD45	Human	Hematopoietic Cell Marker	BD Biosciences	Lymphocytes, Macrophages, Dendritic Cells
EpCAM	Human	Epithelial Cell Marker	BD Biosciences	Alveolar Type I and II Cells
CD163	Human	Activated/Anti-Inflammatory Macrophages	BD Biosciences	Macrophages and Monocytes
ACE2	Human	ACE2 Receptor Marker	R&D Systems	Alveolar Type II Cells, Macrophages, Endothelial Cells

4.0 Results

4.1 Aim 1: Generate a Wuhan Strain SARS-CoV-2 Pseudotyped Lentivirus Capable of Infecting Human Lung Cells in Suspension

4.1.1 Infection of Vero E6 ACE2/TMPRSS2 to Understand Efficiency of SARS-CoV-2 Pseudotyped Lentivirus

In order to test efficiency of Wuhan strain SARS-CoV-2 pseudotyped lentivirus, we infected vero E6 cells that are modified to express human ACE2/TMPRSS2. Images were taken at 48 hours post-infection to assess mCherry signal at peak expression (Figure 4). In vero E6 cells that express ACE2/TMPRSS2 infected with the SARS-CoV-2 pseudotyped lentivirus, there is some mCherry signal present, indicating infection (Figure 4A). We created an empty vector pseudotyped lentivirus using the same protocol used for the SARS-CoV-2 pseudotyped lentivirus, but we omitted the SARS-CoV-2 spike plasmid. We then used it to infect the vero E6 cells that express ACE2/TMPRSS2. There is no mCherry signal present without the SARS-CoV-2 spike present (Figure 4B). Next, we used the SARS-CoV-2 pseudotyped lentivirus to infect normal vero E6 cells that do not express ACE2/TMPRSS2. There is no mCherry signal without the host receptors present (Figure 4C).

We then compared 12 images in one well in a 6-well plate from each treatment group in NIS-Elements to determine the mCherry positive cell density in each group. Images from the vero E6 cells that express ACE2/TMPRSS2 infected with the SARS-CoV-2 pseudotyped lentivirus had a range of 1.99-72.39$\mu m^2/pixel^2$ with a mean of 17.15$\mu m^2/pixel^2$, while the other treatment groups

had a mean of 0.021μm^2/pixel^2 and 0.020μm^2/pixel^2 respectively (Figure 4D). Lastly, we analyzed the vero E6 cells that expressed ACE2/TMPRSS2 under SARS-CoV-2 pseudotyped lentivirus infection and mock conditions using flow cytometry. Both treatment groups had low levels of ACE2 expression; 1.85% of the infected sample expressed ACE2, and 1.12% of the mock sample expressed ACE2. In the population of ACE2 expressing cells in the infected vero E6 cells, 13.2% of that population expressed mCherry, indicating expression. While only 1.27% of the ACE2 expressing vero E6 cells expressed mCherry in the mock infected cells (Figure 5).

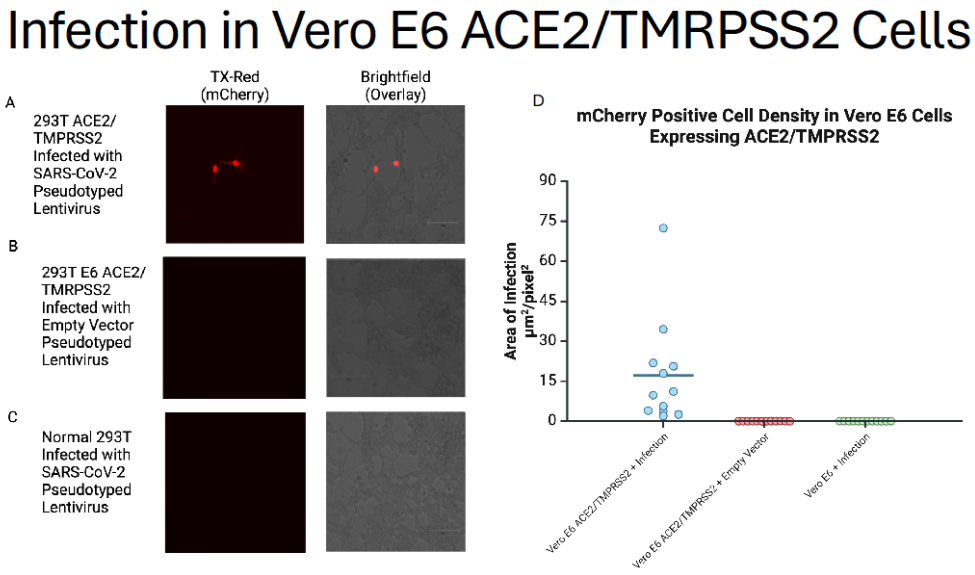

Figure 4 Infection of Vero E6 Cells that Express Human ACE2/TMPRSS2

Fluorescent microscopic imaging 48 hours post infection in vero E6 cells that express ACE2/TMPRSS2 infected with SARS-CoV-2 pseudotyped Lentivirus (A), vero E6 cells that express ACE2/TMPRSS2 infected with an empty vector pseudotyped lentivrus (B), and vero E6 cells that do not express ACE2/TMPRSS2 infected with SARS-CoV-2 pseudotyped lentivirus (C). Using NIS-Elements to quantify mCherry signal 48 hours post infection in Vero E6 Cells expressing ACE2/TMPRSS2 infected with SARS-CoV-2 pseudotyped lentivirus, an empty vector lentivirus, and normal Vero E6 cells infected with the pseudotyped virus (D). Created with Biorender.com

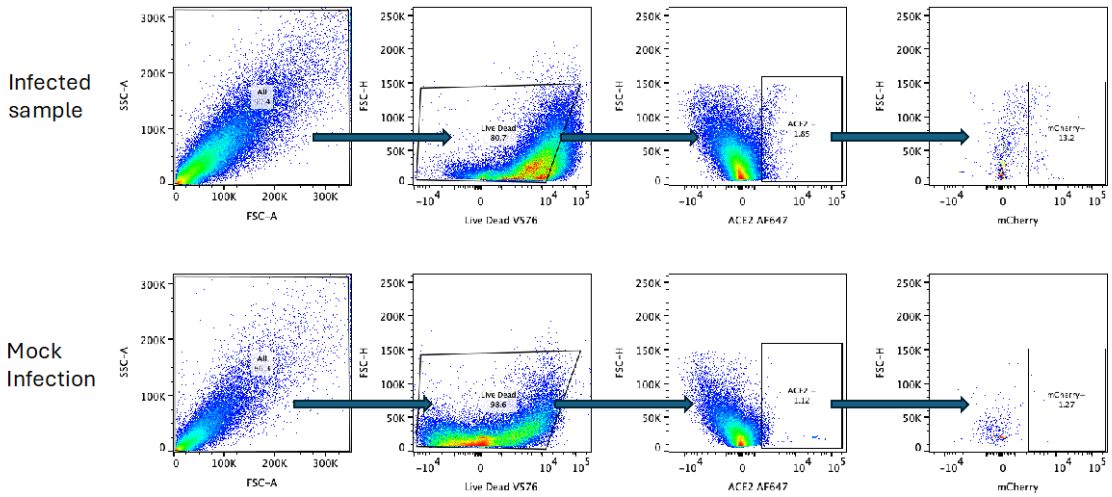

Figure 5 Flow Cytometry Vero E6 Cells Expressing ACE2/TMPRSS2

Flow Cytometry ran 48 hours post infection on vero E6 cells expressing ACE2/TMPRSS2 infected with SARS-CoV-2 pseudotyped lentivirus and mock infection staining for ACE2.

4.1.2 Infection of 293T Cells that Express Human ACE2/TMPRSS2 to Understand Viral Efficiency

Due to the low level of mCherry signal and ACE2 expression observed in the vero E6 cells, we infected 293T cells under the same conditions and observed mCherry signal at 48 hours post infection using fluorescent microscopic imaging and flow cytometry. We infected 293T cells that express ACE2/TMPRSS2 with the Wuhan strain SARS-CoV-2 pseudotyped lentivirus, and we did observe some mCherry signal indicating infection in the images taken at 48 hours post infection (Figure 6A). In 293T cells that express ACE2/TMPRSS2 infected with the empty vector

pseudotyped lentivirus, no mCherry signal was observed (Figure 6B). No mCherry signal was observed in the normal 293T cells that do not express ACE2/TMPRSS2 as well (Figure 6C).

We then compared 12 images from one 6-well plate for each treatment group using NIS-Elements to determine mCherry positive cell density for the 293T cells. Images for the 293T cells that express ACE2/TMPRSS2 that were infected with the Wuhan strain SARS-CoV-2 pseudotyped lentivirus had a smaller range from 0.032-13.69$\mu m^2/pixel^2$ with a mean of 5.08$\mu m^2/pixel^2$. While both of the other treatment groups had a mean of 0.04$\mu m^2/pixel^2$ (Figure 6D). Last, we compared 293T cells that express ACE2/TMPRSS2 infected with the Wuhan strain SARS-CoV-2 pseudotyped lentivirus and a mock infected group using flow cytometry. In the infected 293T cells that express ACE2/TMPRSS2, 85.9% of the sample expressed ACE2; however, only 1.01% of that population expressed mCherry signal. In the mock 293T ACE2/TMPRSS2 cells, 91.3% of that sample expressed ACE2, and 1.21% of that population expressed mCherry (Figure 7).

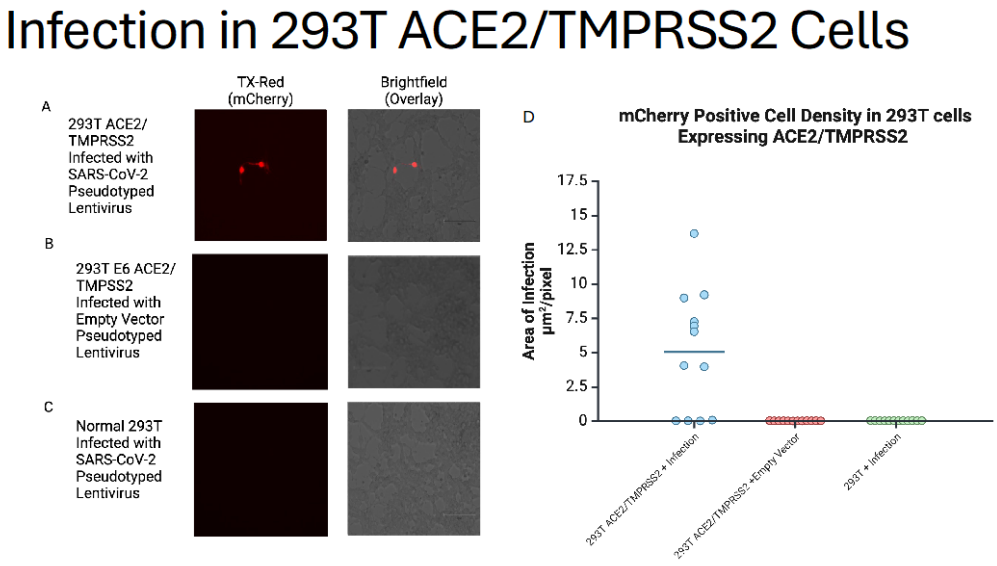

Figure 6 Infection of 293T Cells that Express Human ACE2/TMPRSS2

Fluorescent microscopic imaging 48 hours post infection in 293T cells that express ACE2/TMPRSS2 infected with SARS-CoV-2 pseudotyped Lentivirus (A), 293T cells that express ACE2/TMPRSS2 infected with an empty vector pseudotyped lentivrus (B), and 293T cells that do not express ACE2/TMPRSS2 infected with SARS-CoV-2 pseudotyped lentivirus (C), using NIS-Elements to quantify mCherry signal 48 hours post infection in 293T Cells expressing ACE2/TMPRSS2 infected with SARS-CoV-2 pseudotyped lentivirus, an empty vector lentivirus, and normal 293Tcells infected with the pseudotyped lentivirus (D). Created with Biorender.com

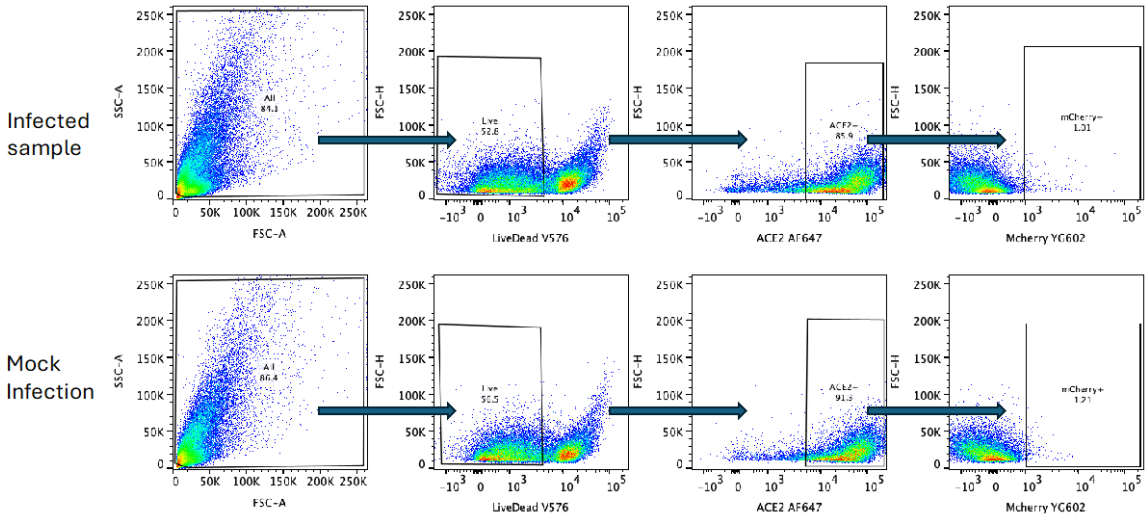

Figure 7 Flow Cytometry 293T Cells Expressing ACE2/TMPRSS2

Flow Cytometry ran 48 hours post infection on 293T cells expressing ACE2/TMPRSS2 infected with SARS-CoV-2 pseudotyped lentivirus and mock infection staining for ACE2.

4.2 Aim 2: The infection of Human Lung Cell Suspensions with the Wuhan Strain SARS-CoV-2 Pseudotyped Lentivirus

4.2.1 Microscopic Imaging and Flow Cytometry of Human Lung Cell Suspensions Infected with the SARS-CoV-2 Pseudotyped Lentivirus

Table 2 Human Lung Donor Information

Identification	Age	Sex	Health History
AHLO126	57	F	Hypertension, Diabetes

AICZ395	52	M	Hypertension
AIBW239	56	M	Hypertension

In addition to testing cell lines expressing human ACE2/TMPRSS2, we infected human lung cells in suspension from rejected organ donors (Table 2) to determine the tropism of the Wuhan strain SARS-CoV-2 pseudotyped lentivirus. To observe infection, we relied on the mCherry fluorescent marker to indicate cell entry and stained the samples with dapi. There is more mCherry expression in the infected human lung cell suspensions than the mock. There is slight autofluorescence visible in the mock infected TX-Red channel, but it is not bright enough to indicate infection (Figure 8A, 8B). However, expression of both mCherry and dapi varied from donor to donor. In the NIS-Elements analysis, there is a clear difference in mCherry positive cell density between donors and infection groups. In donor AICZ395, the infection group has a mean of 32.81$\mu m^2/pixel^2$ while the mock treatment for that same donor is 0.024$\mu m^2/pixel^2$. The mean mCherry positive cell density for the donor AIBW239 is 2.17$\mu m^2/pixel^2$ in the infection group, and 0.027$\mu m^2/pixel^2$ in the mock treatment group. The donor AHLO126 has a mean mCherry positive cell density of 0.94$\mu m^2/pixel^2$ in the infected treatment group and 0.057$\mu m^2/pixel^2$ in the mock treatment group (Figure 9).

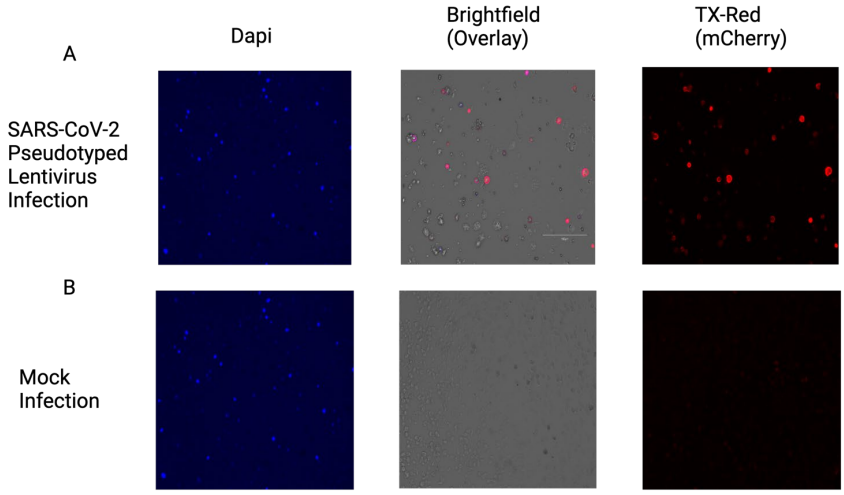

Figure 8 Infection of Human Lung Cell Suspensions

Fluorescent microscopic imaging 48 hours post infection in human lung cell suspensions infected with SARS-CoV-2 pseudotyped Lentivirus (A) and mock group (B) stained with dapi. Created with Biorender.com

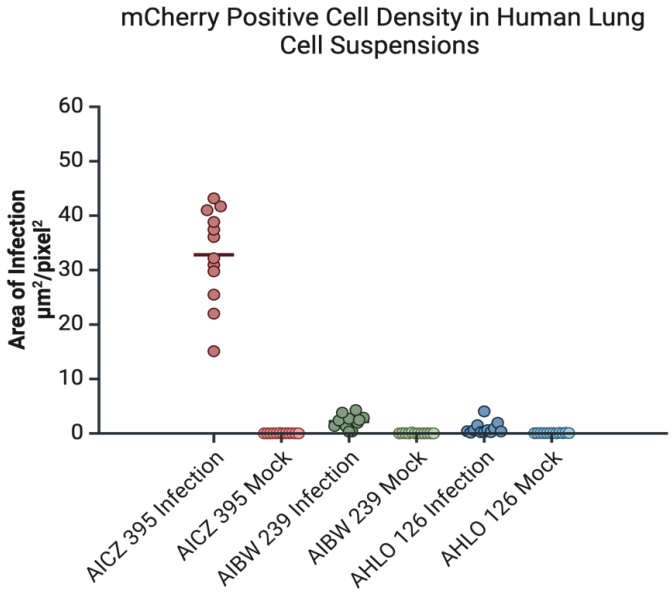

Figure 9 mCherry Positive Cell Density in Human Lung Cell Suspensions

Using NIS-Elements to quantify mCherry signal 48 hours post infection in human lung cell suspensions infected with SARS-CoV-2 pseudotyped lentivirus, and mock infection. Created with Biorender.com

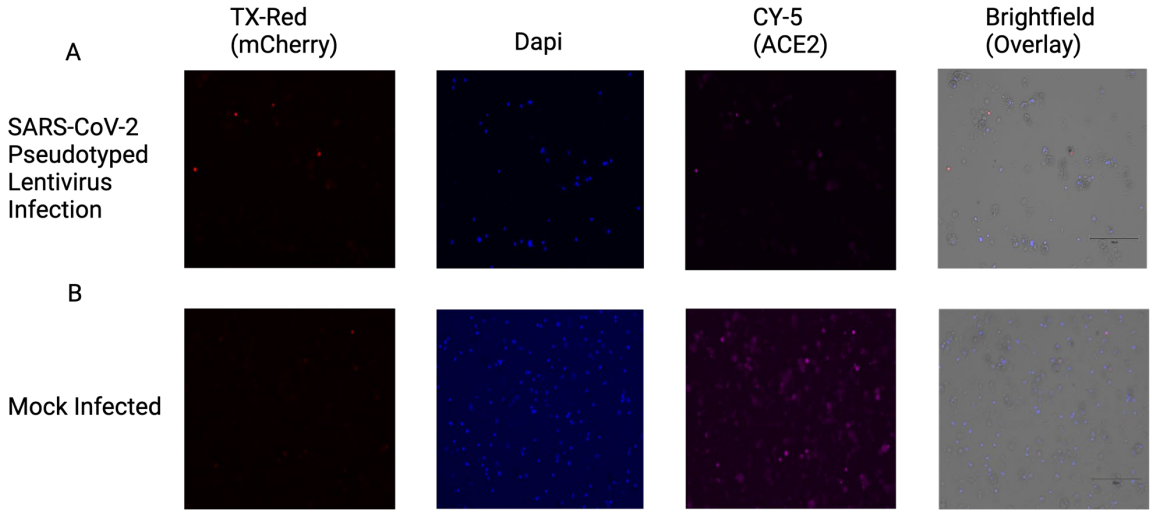

Figure 10 Infection of Human Lung Cell Suspensions and ACE2 Staining

Fluorescent microscopic imaging 48 hours post infection in human lung cell suspensions infected with SARS-CoV-2 pseudotyped Lentivirus (A) and mock group (B) stained with ACE2 dapi. Created with Biorender.com

In an attempt to observe overlap in cells in the human lung cell suspensions that were infected with the Wuhan strain SARS-CoV-2 pseudotyped lentivirus and expressed ACE2, we used an ACE2 antibody for immunofluorescence staining and flow cytometry. This antibody has not previously been used for immunofluorescence staining, so the results were not as expected and possibly impacted mCherry expression. There is expression of both ACE2 in the CY-5 channel and mCherry in the TX-Red channel in the donor AICZ395 when infected with the SARS-CoV-2

pseudotyped lentivirus, but ACE2 appears brighter in the mock sample (Figure 10). Other donors do not express the stain.

We then ran flow cytometry on the human lung cell suspensions infected with the Wuhan strain SARS-CoV-2 pseudotyped lentivirus and stained for CD45, EpCAM, CD163, ACE2 and gated for mCherry expression from the virus. Each donor varied between cell types and infection levels, but we experienced difficulty staining for ACE2. We had a limited supply of human lung cell suspensions, so we could not troubleshoot or optimize the protocol for ACE2 staining. The results were not as expected. In the donor AHLO126 infected with SARS-CoV-2 pseudotyped lentivirus, only 7.49% of the live cells expressed ACE2 and only 2.31% of that total population expressed mCherry. While in the same donor for the mock infected sample, 2.59% of the live cells expressed ACE2, and 1.60% of that total population expressed mCherry (Figure 11).

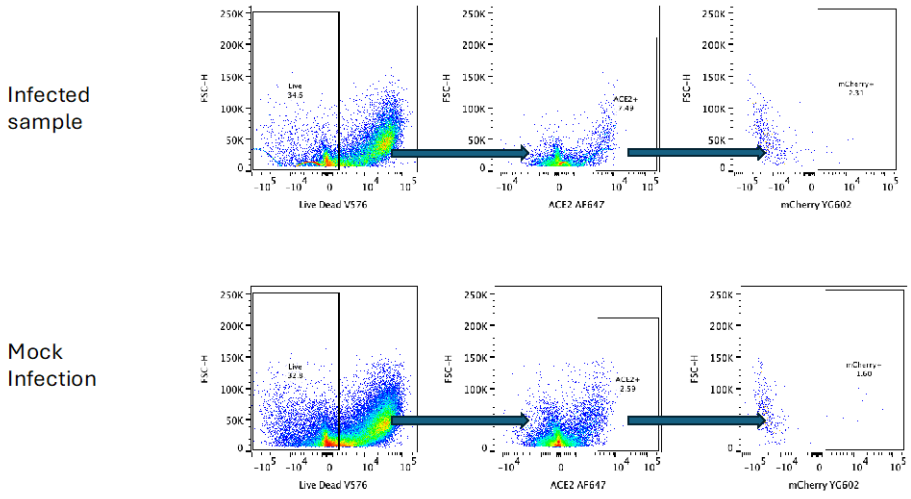

Figure 11 ACE2 Expression in Human Lung Cell Suspensions Infected with SARS-CoV-2 Pseudotyped Lentivirus

Flow Cytometry ran 48 hours post infection on human lung cell suspensions infected with SARS-CoV-2 pseudotyped lentivirus and stained ACE2 and mock infection.

Even though we were unable to rely on the ACE2 antibody for flow cytometry, we classified the cell types using a Live/Dead stain, CD45, EpCAM, and CD163. Donor AHLO126 had 36.8% of the live cells express CD45, 2.35% of the live cells that were CD45- expressed EpCAM, and 61.3% of the CD45+ cells were macrophages (Figure 12,13). In donor AICZ395, 32.4% of live cells expressed CD45, 15.4% of the live cells that were CD45- expressed EpCAM, 45.6% of the CD45+ cells were macrophages, and in donor AIBW239, 30.5% of living cells expressed CD45, 46.7% of live cells that were CD45- expressed EpCAM, 33.8% of the CD45+ population were macrophages (Figure 13).

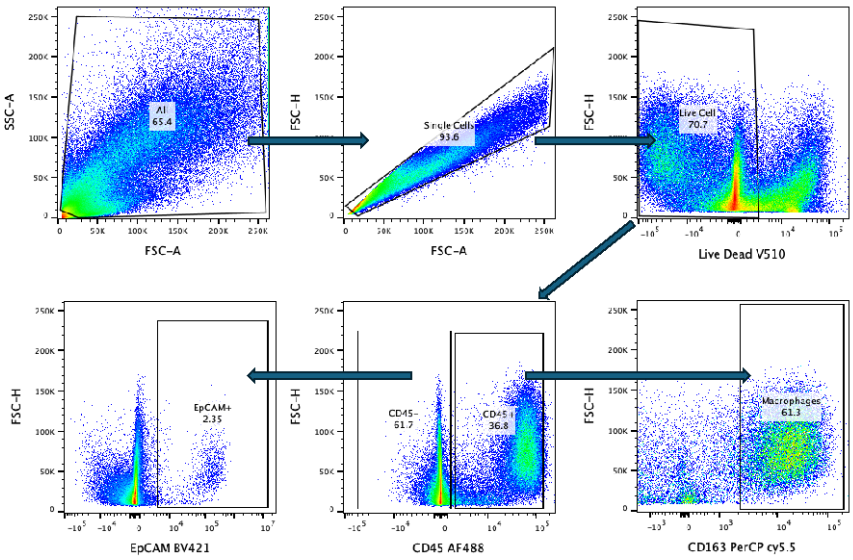

Figure 12 Flow Cytometry on Uninfected Human Lung Cell Suspensions

Flow cytometry ran on uninfected human lung cell suspensions stained with a live/dead stain, CD45, EpCAM, and CD163.

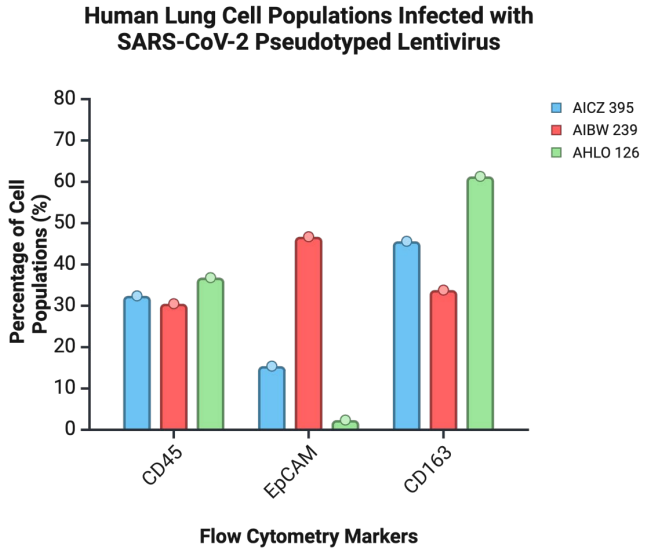

Figure 13 Populaiton Percentages of Uninfected Human Lung Cell Suspensions

Population percentages from Flow Cytometry of cells expressing CD45 from the live cell population, and percentages of cells gated from CD45 that express EpCAM and CD163.

We then wanted to examine these same cell populations in human lung cell suspensions infected with the SARS-CoV-2 pseudotyped lentivirus using flow cytometry. Once again there was variation between cell populations and infection levels between donors, but they were similar to the populations in the uninfected sample. Donor AHLO126 had only 11.6% of the live cells express CD45, 1.61% of the live cells that were CD45- expressed EpCAM, and 39.8% of the CD45+ cells were macrophages, and 29.0% of the live cells expressed mCherry (Figure 14). In donor AIBW239, 41.8% of living cells expressed CD45, 31.3% of live cells that were CD45- expressed EpCAM, 32.7% of the CD45+ population were macrophages, and 5.48% of live cells expressed mCherry. In donor AICZ395, 25.8% of live cells expressed CD45, 12.7% of the live cells that were CD45- expressed EpCAM, 44.7% of the CD45+ cells were macrophages, and in this sample 3.71% of the live cells expressed mCherry (Figure 15).

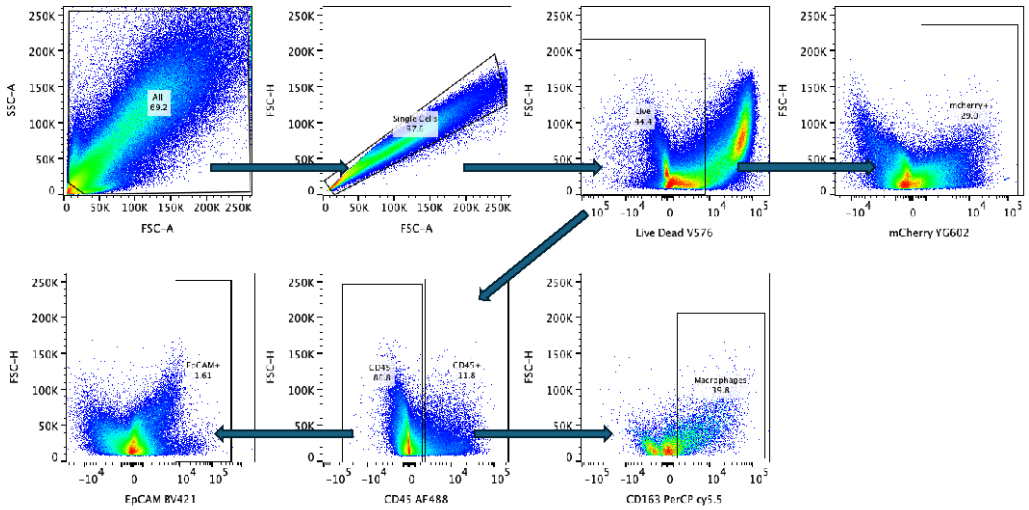

Figure 14 Flow Cytometry Human Lung Cell Suspensions Infected with SARS-CoV-2 Pseudotyped Lentivirus

Flow cytometry ran 48 hours post infection on human lung cell suspensions stained with a live/dead stain, CD45, EpCAM, and CD163.

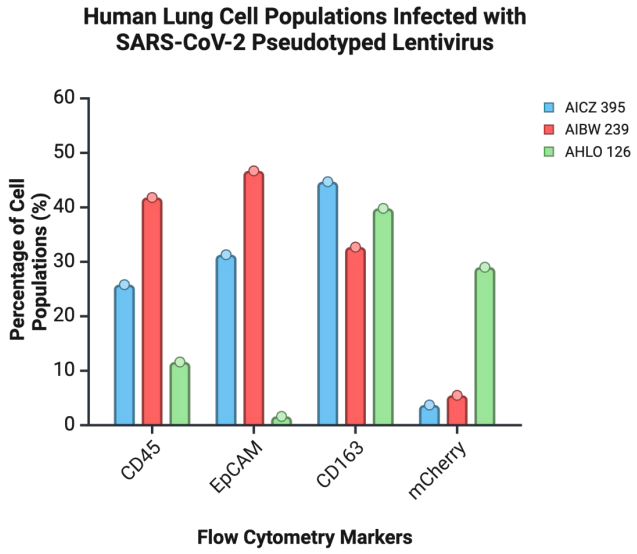

Figure 15 Populaiton Percentages of Infected Human Lung Cell Suspensions

Population percentages from Flow Cytometry of cells expressing CD45 from the live cell population, and percentages of cells gated from CD45 that express EpCAM and CD163. mCherry population is gated from live cells.

Using the same flow cytometry experiment, we were able to use FlowJo to gate mCherry signal from the EpCAM+ populations for each donor (Figure 16). In donor AHLO126, 56.3% of EpCAM+ cells expressed mCherry, in donor AIBW239, 72.0% of EpCAM+ cells expressed mCherry, and in AICZ395, 11.1% of EpCAM+ cells expressed mCherry (Figure 17).

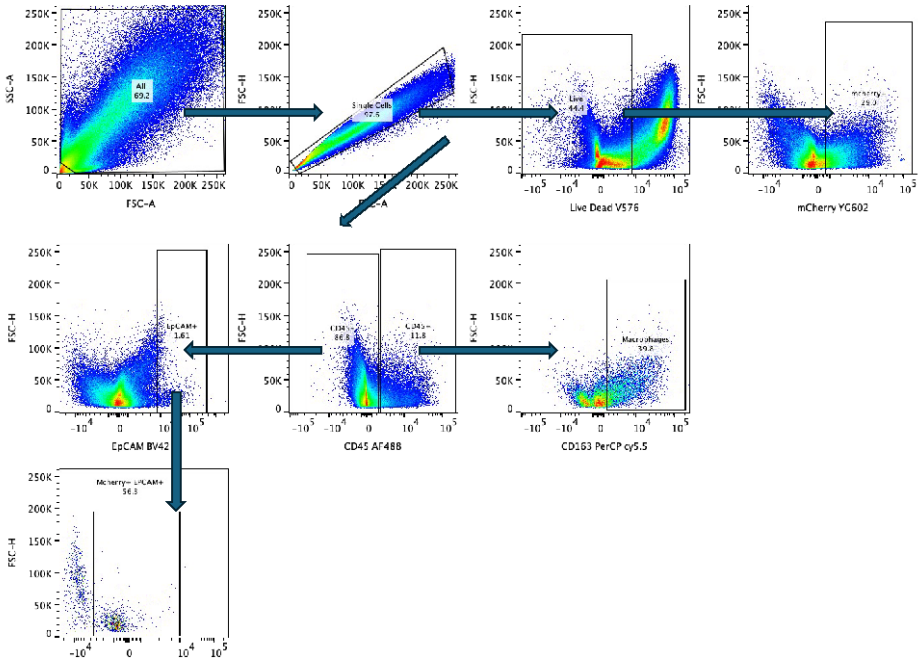

Figure 16 mCherry Signal Using Flow Cytometry in Human Lung Cell Suspensions Infected with SARS-CoV-2 Pseudotyped Lentivirus

Flow cytometry ran 48 hours post infection on human lung cell suspensions stained with a live/dead stain, CD45, EpCAM, CD163, and mCherry gated from the EpCAM+ population.

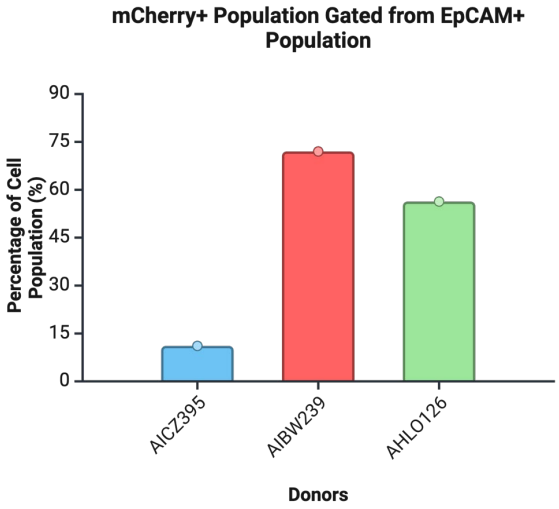

Figure 17 EpCAM+mCherry+ Percentages of Infected Human Lung Cell Suspensions

mCherry expression in EpCAM+ cell populations in each infected donor 48 hours post infection.

Finally, using FlowJo, we gated CD45, EpCAM, and CD163 cell populations in each infected donor from the mCherry+ population from live cells (Figure 18). We focused on the EpCAM+ and CD163+ populations gated directly from the mCherry+ populations. In donor AICZ395, 21.4% of mCherry+ were also EpCAM+, and 33.8% of the mCherry+ population also expressed CD163. In donor AIBW239, 27.5% of the mCherry+ population also expressed EpCAM, and 30.8% of the mCherry+ population expressed CD163. In donor AHLO126, 13.1% of the mCherry population expressed EpCAM, and 17.8% of the mCherry population expressed CD163 (Figure 19).

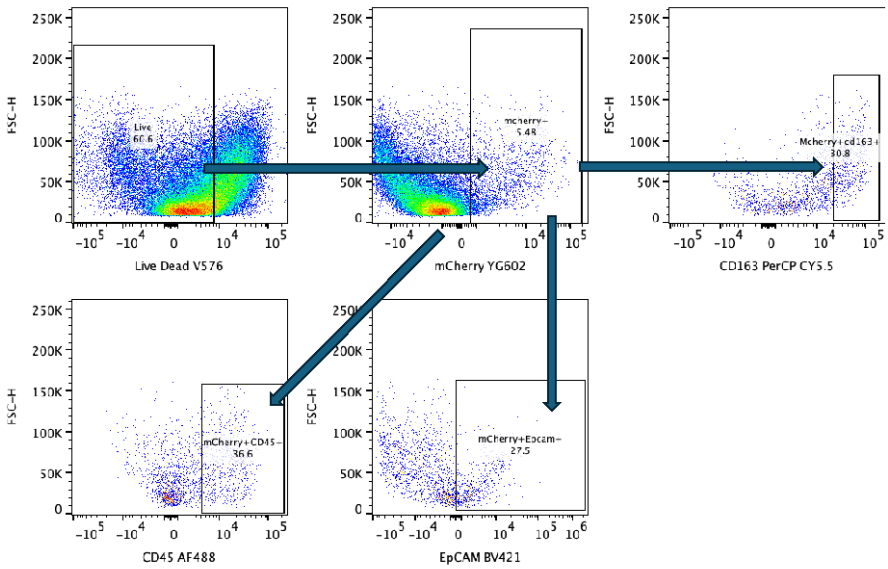

Figure 18 mCherry Population Comparisons Using Flow Cytometry

Flow cytometry ran 48 hours post infection on human lung cell suspensions comparing different cell populations gated from the total amount of mCherry signal in the sample.

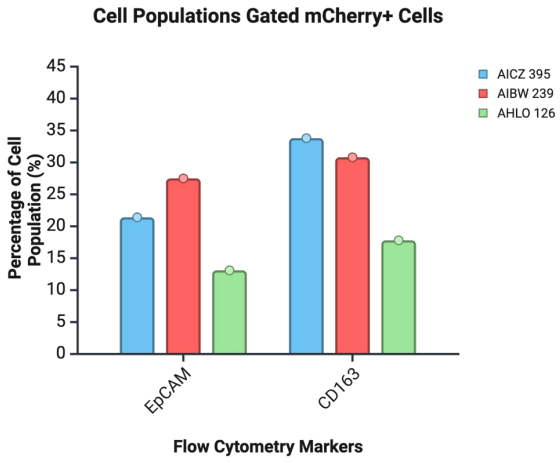

Figure 19 mCherry Population Comparisons Between Donors

Comparison of flow cytometry analysis between donors showing different cell populations in the mCherry+ population gated from live cells.

5.0 Discussion

In aim one, we wanted to determine if we could produce a reliable Wuhan strain SARS-CoV-2 pseudotyped lentivirus by transfecting 293T cells and concentrating the viral particles (Figure 3). Previous studies have found that a SARS-CoV-2 pseudotyped virus is a reliable way to study the virus by neutralization (49,52). The virus functions properly as it is able to infect susceptible cells that express ACE2/TMRPSS2 and has a titer of at least $1.5X10^4$fu/mL, but it does not efficiently infect in vero E6 or 293T cell lines (Figures 4, 6). It is possible to increase the efficiency of the pseudotyped virus by creating larger stocks at a time and optimizing each step. However, the issue may stem from the cell lines (51). Depending on the transfection kit and delivery system, all cell lines are not as susceptible to infection (49). It is also possible that the efficiency was higher than predicted, and the reason for low mCherry signal was due to the amount of cell death present. There are major differences in the two cell lines observed in this study. The level of ACE2 is lower in vero E6 cells than in 293T cells. In the infected vero E6 cells, only 1.85% of the population expressed ACE2, but 13.2% of that total population was infected (Figure 5). The infected 293T cells had 85.9% expression of ACE2 in the live population, but only 1.01% of that population expressed mCherry (Figure 7).

While the pseudotyped virus is not as efficient in the observed cell lines, it does clearly show that the spike protein is both necessary and sufficient for infection (4). There is increased mCherry signal in both vero E6 and 293T cells that express ACE2/TMPRSS2, and there is no infection in the cell lines that do not express ACE2/TMPRSS2. This proves that the SARS-CoV-2 spike protein is present on this virus and needed for infection. Also, in both cell lines that express ACE2/TMPRSS2 there is no mCherry signal present, showing that the spike protein needs to bind

to those receptors in order to enter the host cell (Figure 4-7) (3,10). The pseudotyped virus does work, and it is able to infect cell lines expressing ACE2/TMPRSS2. More steps will be needed to optimize its efficiency.

COVID-19 has a wide range of symptoms and effects individuals differently. Some individuals will be infectious but never show symptoms, while others develop severe disease (2,19). In aim two we wanted to determine the tropism of the Wuhan strain SARS-CoV-2 pseudotyped lentivirus in human lung cell suspensions, so we infected human lung cell suspensions from three different donors with the SARS-CoV-2 pseudotyped lentivirus to observe viral entry. Using microscopic fluorescent imaging, we were able to observe mCherry signal from the SARS-CoV-2 pseudotyped lentivirus in the infected human lung cell suspensions (Figure 8).

However, when quantifying the images using NIS-Elements, it was clear that not all donors were as susceptible to the virus as others. The donor AICZ395 had an mCherry positive cell density of $32.81 \mu m^2/pixel^2$, but the other two donors had very low mCherry positive cell density (Figure 9). Many factors could play a part in viral entry of the SARS-CoV-2 pseudotyped lentivirus. Once again, we must consider the efficiency of the viral particles. The donor AICZ395 has a higher mCherry positive cell density than the vero E6 and 293T cells that express ACE2/TMRPSS2, so it is clear that the virus can infect the human lung cell suspensions. Another factor could be the variation between individuals and comorbidities (15,39). All donors in this study were 52-57 years old and had at least one other existing medical condition such as diabetes or hypertension. Donor AHLO126 was female and donors AICZ395 and AIBW239 were male. We do not know the vaccination status of these individuals. Lastly, ACE2 expression and other susceptible cell types also varies from donor to donor, making it harder for viral entry (36).

In attempts to better observe ACE2's role in viral entry, we used an ACE2 antibody for immunofluorescence staining and flow cytometry. This antibody was not marketed for immunofluorescence staining. We were able to detect signal in the donor AICZ395 but not in AHLO126 or AIBW239. However, in the sample infected with the SARS-CoV-2 pseudotyped lentivirus and stained with ACE2, the signal for mCherry and dapi were not as bright compared to the mock infected sample (Figure 10). SARS-CoV-2 infection does cause cell damage and downregulates ACE2 (47). However, the pseudotyped lentivirus is replication incompetent, and it should not cause cell death, but it could still downregulate ACE2. Interestingly, when we used the ACE2 antibody for flow cytometry, the sample infected with the SARS-CoV-2 pseudotyped lentivirus expressed higher levels of ACE2 than the mock infection sample did (Figure 11). Future steps must be taken to optimize ACE2 immunofluorescence staining and flow cytometry in order to have a more complete understanding.

Using flow cytometry to analyze SARS-CoV-2 infection in the donors, we were also able to observe how widely cell populations and infection differ (Figure 12). Each donor had different ranges of CD45, EpCAM, and CD163 expressed, and interestingly, the donor AHLO126 had the lowest percentage of EpCAM expressed but the highest percentage of mCherry expressed (Figure 13-15). Alveolar type II cells are known to be the main target for natural SARS-CoV-2, but there are other cells that express ACE2 in the lungs, and there are other proteins capable of viral entry such as CD147. There is a high level of mCherry signal in the macrophage populations as well, indicating that human alveolar macrophages are susceptible to SARS-CoV-2 infection, and they play a more important role than expected at the start of this project (Figures 16-19).

In conclusion, the Wuhan strain SARS-CoV-2 pseudotyped lentivirus model does work to infect susceptible cell lines and human lung cell suspensions. The spike protein pseudotyped onto

the lentiviral particles is necessary and sufficient for viral entry, and in the susceptible cell lines, ACE2/TMPRSS2 receptor is needed for infection. There is viral entry in human lung cell suspensions, however, infection varies from donor to donor. Donors also have divergence in total cell type overall. Lastly, while literature supports the idea that alveolar type II epithelial cells are the main target of SARS-CoV-2 infection, it is clear that alveolar macrophages are also susceptible and play a role in viral entry.

6.0 Future Directions

After optimizing protocols to create a more efficient pseudotyped lentivirus and more accurate methods to analyze results, there are a few possibilities for this study. One possibility would be to repeat this experiment on archived human lung cell suspensions from before 2019 in order to see what differences in infection of naïve lung cell suspensions would occur.

New SARS-CoV-2 variants are emerging, and in order to fully understand the virus, it is necessary to have access to study variant strains. Creating pseudotyped lentiviruses for current circulating strains of SARS-CoV-2 will allow more researchers to study the virus, which could lead to better therapeutic options and possibly better vaccines. Emergency preparedness is vital for the healthcare system, and being able to work with different strains of this virus safely and reliably in a biosafety level two setting could lower the burden on the healthcare system and save lives.

Additionally, this research could be expanded to observe different pathways for SARS-CoV-2 infection. The spike protein binding to ACE2 is known to be the main route for infection in humans, but the virus has other options for infection. By blocking ACE2, the SARS-CoV-2 pseudotyped lentiviruses could be used to determine which infected cells in suspension are expressing CD147. This is specifically important for creating better therapeutic options. Lastly, the results of these studies could be compared to the wild-type virus to determine how reliable the SARS-CoV-2 pseudotyped lentivirus model works.

7.0 Public Health Significance

With the circulation of new variants of SARS-CoV-2, it is expected that COVID-19 will continue to impact people's lives. In the United States alone, many adults are not completely vaccinated, and some are still hesitant to be vaccinated at all (24). This allows for further circulation of the virus and more chance for the virus to mutate. These mutations could cause the virus to be able to spread faster or be resistant to current therapeutics and vaccines. In addition to more cases, researchers still do not have a full understanding of Long COVID, and therefore cannot properly help those patients struggling with prolonged illness (17).

Using SARS-CoV-2 pseudotyped lentiviruses to deepen our understanding of both the virus and the disease is essential. It allows more researchers at lower containment levels the opportunity to observe the virus, which could lead to better understands of interactions between cell types and the virus and host cells. A deeper understanding from more individuals will lead to better scientific communication to the public, better therapeutics, and a better emergency response in the future.

Bibliography

1. Ludwig, S, Zarbock, A. 2020. Coronaviruses and SARS-CoV-2: A Brief Overview. 131:93. doi: 10.1213/ANE.0000000000004845. https://journals.lww.com/anesthesia-analgesia/FullText/2020/07000/Coronaviruses_and_SARS_CoV_2__A_Brief_Overview.14.aspx.

2. Sternberg, A. Structural features of coronavirus SARS-CoV-2 spike protein: Targets for vaccination - ScienceDirect. . https://www.sciencedirect.com/science/article/pii/S0024320520308079.

3. Jackson, CB, Farzan, M, Chen, B, Choe, H. 2022. Mechanisms of SARS-CoV-2 entry into cells. Nat Rev Mol Cell Biol. 23:3-20. doi: 10.1038/s41580-021-00418-x. https://www-nature-com.pitt.idm.oclc.org/articles/s41580-021-00418-x.

4. Viruses | Free Full-Text | Protocol and Reagents for Pseudotyping Lentiviral Particles with SARS-CoV-2 Spike Protein for Neutralization Assays. . https://www.mdpi.com/1999-4915/12/5/513.

5. Mani, S., & Weitkamp, J.-H. (Eds.). (2024). Textbook of SARS-COV-2 and COVID-19 : epidemiology, pathophysiology, immunology, clinical manifestations, treatment, complications, and preventive measures. Elsevier.

6. Kim, D, Lee, J, Yang, J, Kim, JW, Kim, VN, Chang, H. 2020. The architecture of SARS-CoV-2 transcriptome. 181:914-921. e10.

7. The SARS-CoV-2 outbreak: What we know - ScienceDirect. . https://www.sciencedirect.com/science/article/pii/S1201971220301235#sec0010.

8. Atkinson, J, Chartier, Y, Pessoa-Silva, CL, Jensen, P, Li, Y, Seto, W. 2009. Respiratory droplets. World Health Organization. https://www.ncbi.nlm.nih.gov/books/NBK143281/.

9. Zhang, J. Structure of SARS-CoV-2 spike protein - ScienceDirect. . https://www.sciencedirect.com/science/article/pii/S1879625721000973.

10. Hartenian, E, Nandakumar, D, Lari, A, Ly, M, Tucker, JM, Glaunsinger, BA. 2020. The molecular virology of coronaviruses. J.Biol.Chem. 295:12910-12934.

11. SARS-CoV-2 pathogenesis | Nature Reviews Microbiology. . https://www.nature.com/articles/s41579-022-00713-0.

12. WHO COVID-19 Dashboard (Circulation). 2024. https://data.who.int/dashboards/covid19/circulation?n=c

13. COVID-19 Map. 2024:. https://coronavirus.jhu.edu/map.html.

14. Dix, E., & Roy, K. (2022). COVID-19. The Psychiatric Clinics of North America, 45(4), 625–637. https://doi.org/10.1016/j.psc.2022.07.009

15. COVID-19 and Your Health. 2024:. https://www.cdc.gov/coronavirus/2019-ncov/your-health/about-covid-19.html.

16. Estimate the incubation period of coronavirus 2019 (COVID-19) - ScienceDirect. . https://www.sciencedirect.com/science/article/pii/S0010482523002597.

17. Sudre, CH, Murray, B, Varsavsky, T, Graham, MS, Penfold, RS, Bowyer, RC, Pujol, JC, Klaser, K, Antonelli, M, Canas, LS, Molteni, E, Modat, M, Jorge Cardoso, M, May, A, Ganesh, S, Davies, R, Nguyen, LH, Drew, DA, Astley, CM, Joshi, AD, Merino, J, Tsereteli, N, Fall, T, Gomez, MF, Duncan, EL, Menni, C, Williams, FMK, Franks, PW, Chan, AT, Wolf, J, Ourselin, S, Spector, T, Steves, CJ. 2021. Attributes and predictors of long COVID. Nat Med. 27:626-631. doi: 10.1038/s41591-021-01292-y. https://www-nature-com.pitt.idm.oclc.org/articles/s41591-021-01292-y.

18. Meyerowitz, EA, Richterman, A, Bogoch, II, Low, N, Cevik, M. 2021. Towards an accurate and systematic characterisation of persistently asymptomatic infection with SARS-CoV-2. 21:e163-e169.

19. Eckerle, I, Meyer, B. 2020. SARS-CoV-2 seroprevalence in COVID-19 hotspots. 396:514-515.

20. Coronavirus Disease 2019 (COVID-19). 2024:. https://www.cdc.gov/coronavirus/2019-ncov/variants/variant-surveillance.html.

21. WHO COVID-19 Dashboard (Variants). 2024. https://data.who.int/dashboards/covid19/variants?n=c

22. COVID-19 Vaccination. 2024:. https://www.cdc.gov/coronavirus/2019-ncov/vaccines/stay-up-to-date.html.

23. Vaccines | Free Full-Text | Factors Associated with COVID-19 Vaccine Hesitancy. . https://www.mdpi.com/2076-393X/9/3/300.

24. Frontiers | COVID-19 Vaccine Hesitancy in the United States: A Systematic Review. . https://www.frontiersin.org/journals/public-health/articles/10.3389/fpubh.2021.770985/full.

25. COVID-19 Treatment and Preventive Medication | CDC. . https://www.cdc.gov/coronavirus/2019-ncov/your-health/treatments-for-severe-illness.html.

26. Amani, B, Amani, B. 2023. Efficacy and safety of nirmatrelvir/ritonavir (Paxlovid) for COVID-19: a rapid review and meta-analysis. J.Med.Virol. 95:e28441.

27. Focosi, D, Franchini, M, Maggi, F, Shoham, S. 2024. COVID-19 therapeutics. Clin.Microbiol.Rev. 119.

28. The Human Lung Cell Atlas: A High-Resolution Reference Map of the Human Lung in Health and Disease | American Journal of Respiratory Cell and Molecular Biology. . https://www.atsjournals.org/doi/full/10.1165/rcmb.2018-0416TR.

29. Franks, TJ. Resident Cellular Components of the Human Lung | Current Knowledge and Goals for Research on Cell Phenotyping and Function | Proceedings of the American Thoracic Society. https://www.atsjournals.org/doi/full/10.1513/pats.200803-025HR.

30. A molecular cell atlas of the human lung from single-cell RNA sequencing | Nature. . https://www.nature.com/articles/s41586-020-2922-4.

31. Cell Number and Cell Characteristics of the Normal Human Lung | American Review of Respiratory Disease. . https://www.atsjournals.org/doi/abs/10.1164/arrd.1982.126.2.332.

32. Differentiated Human Alveolar Epithelial Cells and Reversibility of their Phenotype In Vitro | American Journal of Respiratory Cell and Molecular Biology. . https://www.atsjournals.org/doi/full/10.1165/rcmb.2006-0410OC.

33. Jieru Wang, Rebecca Oberley-Deegan, Shuanglin Wang, Mrinalini Nikrad, C. Joel Funk, Kevan L. Hartshorn, Robert J. Mason; Differentiated Human Alveolar Type II Cells Secrete Antiviral IL-29 (IFN-λ1) in Response to Influenza A Infection1. J Immunol 1 February 2009; 182 (3): 1296–1304. https://doi.org/10.4049/jimmunol.182.3.1296

34. Mason, R.J. (2006), Biology of alveolar type II cells. Respirology, 11: S12-S15. https://doi.org/10.1111/j.1440-1843.2006.00800.x

35. Fiege, JK, Thiede, JM, Nanda, HA, Matchett, WE, Moore, PJ, Montanari, NR, Thielen, BK, Daniel, J, Stanley, E, Hunter, RC. 2021. Single cell resolution of SARS-CoV-2 tropism, antiviral responses, and susceptibility to therapies in primary human airway epithelium. 17:e1009292.

36. Grau-Expósito, J, Perea, D, Suppi, M, Massana, N, Vergara, A, Soler, MJ, Trinite, B, Blanco, J, García-Pérez, J, Alcamí, J, Serrano-Mollar, A, Rosado, J, Falcó, V, Genescà, M, Buzon, MJ. 2022. Evaluation of SARS-CoV-2 entry, inflammation and new therapeutics in human lung tissue cells. PLOS Pathogens. 18:e1010171. doi: 10.1371/journal.ppat.1010171. https://journals.plos.org/plospathogens/article?id=10.1371/journal.ppat.1010171.

37. Frontiers | ACE2 Expression in Organotypic Human Airway Epithelial Cultures and Airway Biopsies. . https://www.frontiersin.org/journals/pharmacology/articles/10.3389/fphar.2022.813087/full.

38. Bourgonje, AR, Abdulle, AE, Timens, W, Hillebrands, J, Navis, GJ, Gordijn, SJ, Bolling, MC, Dijkstra, G, Voors, AA, Osterhaus, AD. 2020. Angiotensin-converting enzyme 2 (ACE2), SARS-CoV-2 and the pathophysiology of coronavirus disease 2019 (COVID-19). J.Pathol. 251:228-248.

39. Sidarta-Oliveira, D, Jara, CP, Ferruzzi, AJ, Skaf, MS, Velander, WH, Araujo, EP, Velloso, LA. 2020. SARS-CoV-2 receptor is co-expressed with elements of the kinin-kallikrein, renin-angiotensin and coagulation systems in alveolar cells. 2020.06.02.20120634. doi: 10.1101/2020.06.02.20120634. https://www.medrxiv.org/content/10.1101/2020.06.02.20120634v2.

40. Multifunctional angiotensin converting enzyme 2, the SARS-CoV-2 entry receptor, and critical appraisal of its role in acute lung injury - ScienceDirect. . https://www.sciencedirect.com/science/article/pii/S075333222031386X?via%3Dihub

41. Mechanism of Ligand Recognition by Human ACE2 Receptor | The Journal of Physical Chemistry Letters. . https://pubs-acs-org.pitt.idm.oclc.org/doi/full/10.1021/acs.jpclett.1c01064.

42. Abassi, Z, Higazi, AAR, Kinaneh, S, Armaly, Z, Skorecki, K, Heyman, SN. 2020. ACE2, COVID-19 Infection, Inflammation, and Coagulopathy: Missing Pieces in the Puzzle. Front Physiol. 11:574753. doi: 10.3389/fphys.2020.574753. https://www.ncbi.nlm.nih.gov/pmc/articles/PMC7573220/.

43. Zhao, P, Praissman, JL, Grant, OC, Cai, Y, Xiao, T, Rosenbalm, KE, Aoki, K, Kellman, BP, Bridger, R, Barouch, DH, Brindley, MA, Lewis, NE, Tiemeyer, M, Chen, B, Woods, RJ, Wells, L. 2020. Virus-Receptor Interactions of Glycosylated SARS-CoV-2 Spike and Human ACE2 Receptor. 28:586-601.e6. doi: 10.1016/j.chom.2020.08.004. https://www-sciencedirect-com.pitt.idm.oclc.org/science/article/pii/S1931312820304571.

44. Drucker, DJ. 2021. Diabetes, obesity, metabolism, and SARS-CoV-2 infection: the end of the beginning. 33:479-498.

45. Cristelo, C. SARS-CoV-2 and diabetes: New challenges for the disease - ScienceDirect. . https://www.sciencedirect.com/science/article/pii/S0168822720304782.

46. Ravichandran, B, Grimm, D, Krüger, M, Kopp, S, Infanger, M, Wehland, M. 2021. SARS-CoV-2 and hypertension. 9:e14800.

47. Mackman, N. Coagulation Abnormalities and Thrombosis in Patients Infected With SARS-CoV-2 and Other Pandemic Viruses | Arteriosclerosis, Thrombosis, and Vascular Biology. .

https://www-ahajournals-org.pitt.idm.oclc.org/doi/full/10.1161/ATVBAHA.120.314514#d1e438.

48. Aid, M, Busman-Sahay, K, Vidal, SJ, Maliga, Z, Bondoc, S, Starke, C, Terry, M, Jacobson, CA, Wrijil, L, Ducat, S. 2020. Vascular disease and thrombosis in SARS-CoV-2-infected rhesus macaques. 183:1354-1366. e13.

49. Tandon, R. Effective screening of SARS-CoV-2 neutralizing antibodies in patient serum using lentivirus particles pseudotyped with SARS-CoV-2 spike glycoprotein | Scientific Reports. . https://www.nature.com/articles/s41598-020-76135-w.

50. Bentley, EM, Mather, ST, Temperton, NJ. 2015. The use of pseudotypes to study viruses, virus sero-epidemiology and vaccination. Vaccine. 33:2955-2962. doi: 10.1016/j.vaccine.2015.04.071. https://www.ncbi.nlm.nih.gov/pmc/articles/PMC7127415/.

51. Duvergé, A, Negroni, M. 2020. Pseudotyping lentiviral vectors: when the clothes make the virus. 12:1311

52. Di Genova, C, Sampson, A, Scott, S, Cantoni, D, Mayora-Neto, M, Bentley, E, Mattiuzzo, G, Wright, E, Derveni, M, Auld, B. 2021. Production, titration, neutralisation and storage of SARS-CoV-2 lentiviral pseudotypes. 11:1-21.